Clinical Presentations, Differential Diagnosis, and Imaging Work-Up of Cerebral Mass Lesions

38

Francesca Benedetta Pizzini, Stefanie Thust, and Hans Rolf Jäger

Contents

This publication is endorsed by: European Society of Neuroradiology (www.esnr.org).

F. B. Pizzini
Neuroradiology, Department of Diagnostics and Pathology, Verona University Hospital, Verona, Italy
e-mail: francesca.pizzini@aovr.veneto.it

S. Thust
Department of Brain, Repair and Rehabilitation, Neuroradiological Academic Unit, UCL Institute of Neurology, London, UK

Lysholm Department of Neuroradiology, National Hospital for Neurology and Neurosurgery, London, UK

Imaging Department, University College London Hospitals, London, UK
e-mail: steffi.thust@nhs.net; s.thust@ucl.ac.uk

F. Barkhof et al. (eds.), *Clinical Neuroradiology*,
https://doi.org/10.1007/978-3-319-68536-6_56

Abstract

A brain mass lesion can have a myriad of etiologies and may present acutely or be of insidious onset. Symptoms are related to the lesion location, degree of tissue swelling, and rapidity of its onset. Neoplasms can arise from a variety of structures, including glial and neuronal cells, the meninges, ventricular elements, and gland tissue; furthermore, a number of somatic metastases may spread to the brain. **Clinical neuroradiology** plays an important role by considering non-neoplastic space occupying brain lesions, ranging from infectious processes (encephalitis, cerebritis, cerebral abscess) to tumefactive demyelination, vascular (arterial and venous infarction), autoimmune (sarcoidosis, Ig4 disease, vasculitis), toxic-metabolic and transient (e.g., postictal swelling) conditions. Tumor mimics are often, but not always identifiable through pattern recognition, using a combination of structural MR imaging sequences and advanced techniques, including follow-up **radiological techniques** where appropriate. Advanced imaging techniques can provide physiological and quantifiable data to aid the distinction of nonneoplastic disease from tumors, as well as the characterization of different brain tumor types. Nonneoplastic entities are discussed in depth in other chapters of this book, but will be briefly addressed where these are relevant in terms of morphological similarities.

H. R. Jäger (✉)
UCL Institute of Neurology, The National Hospital for Neurology and Neurosurgery and University College Hospital (UCH), London, UK

Department of Brain, Repair and Rehabilitation, Neuroradiological Academic Unit, UCL Institute of Neurology, London, UK

Lysholm Department of Neuroradiology, National Hospital for Neurology and Neurosurgery, London, UK

Imaging Department, University College London Hospitals, London, UK
e-mail: r.jager@ucl.ac.uk

Keywords

Brain mass lesions · Tumors · Clinics · Imaging

Abbreviations

ACRIN	American College of Radiology Imaging Network

ADC	Apparent Diffusion Coefficient
APT	Amide Proton Transfer
ASL	Arterial Spin Labeling
BOLD	Blood Oxygen Level-Dependent
CEST	Chemical Exchange Saturation Transfer
Cho	Choline
[^{11}C] Choline	Carbon-11-Choline
CNS	Classification of central nervous system
Cr	Creatine
CSF	Cerebrospinal fluid
CT	Computed Tomography
DCE	Dynamic Contrast Enhanced
DOTA	1,4,7,10-Tetra-azacyclododecane-1,4,7,10-Tetraacetic acid
DTI	Diffusion Tensor Imaging
DSC	Dynamic Susceptibility Contrast
DWI	Diffusion Weighted Imaging
EORTC	European Organisation for Research and Treatment of Cancer
[^{18}F] choline	8F-Fluorinated Choline
[^{18}F] FDG	Fluorodeoxyglucose F 18
FDOPA	[^{18}F]-Dehydroxyphenylalanine
FET	[^{18}F] Fluoroethyl-L-Tyrosine
FLAIR	Fluid-Attenuated Inversion Recovery
fMRI	Functional MRI
Gad	Gadolinium
^{68}Ga-DOTATOC	^{68}Gallium-DOTA-Tyr^3-Octreotide
Glx	Glutamate/Glutamine
HIV	Human Immunodeficiency Viruses
ITSS	Intratumoral Susceptibility Signal
K^{trans}	Transfer Coefficient
MET	[^{11}C]Methionine
MI	Myo-Inositol
MRI	Magnetic Resonance Imaging
MRS	MR spectroscopy
NAA	N-Acetyl Aspartate
NBTS	United States National Brain Tumor Society
PCNSL	Primary Central Nervous System Lymphoma
PET	Positron-Emission Tomography
PNET	Primitive Neuroectodermal Tumor
ppm	Parts per million
PWI	Perfusion-weighted MRI
PXA	Pleomorphic XanthoAstrocytoma
QUIBA	Quantitative Biomarkers Alliance
rCBF	Relative Cerebral Blood Flow
rCBV	Relative Cerebral Blood Volume
T1w	T1-weighted images
T2w	T2-weighted images
TE	Echo Time
TNM	Tumor, node, metastasis
Ve	Extravascular extracellular space
Vp	Plasma volume
WHO	World Health Organisation
3D	Volumetric

Introduction

A brain mass lesion can have a myriad of etiologies and may present acutely or be of insidious onset. Symptoms are related to the lesion location, degree of tissue swelling, and rapidity of its onset. Mass effect occurs either directly, through cell proliferation as true neoplasia, or indirectly through accumulation of fluid (edema), blood products or pus. Brain tumors may also induce surrounding interstitial edema, more commonly in high grade tumors.

Neoplasms can arise from a variety of structures, including glial and neuronal cells, the meninges, ventricular elements, and gland tissue; furthermore, a number of somatic metastases may spread to the brain. The differential of non-neoplastic space occupying brain lesions is wide, ranging from infectious processes (encephalitis, cerebritis, cerebral abscess) to tumefactive demyelination, vascular (arterial and venous infarction), autoimmune (sarcoidosis, Ig4 disease, vasculitis), toxic-metabolic and transient (e.g., postictal swelling) conditions. Tumor mimics are often, but not always identifiable through pattern recognition, using a combination of structural MR imaging sequences and advanced techniques, including

serial follow-up where appropriate. Complexity arises when clinical symptoms are misleading, or where single time point imaging findings are indistinguishable from tumor. Advanced imaging techniques can provide physiological and quantifiable data to aid the distinction of nonneoplastic disease from tumors, as well as the characterization of different brain tumor types.

Epidemiology

Being diagnosed with a brain tumor is a devastating situation for patients, often fraught with periods of uncertainty due to highly variable risk of disease progression. The prognosis differs widely depending on the tumor type; in many cases no cure is achieved so that despite being a rare disease, brain tumors are a leading (20%) cause of death in young adults. In Europe, approximately 80,000 new cases of primary brain tumors are expected each year, with an increase predicted due to greater aging of the population (Crocetti et al. 2012). Predisposing factors are incompletely understood, but known risks include older age, hereditary disposition, and previous radiation exposure.

The most common intracranial tumors are metastases, followed by meningioma and glioma. Approximately 1/3 of newly diagnosed primary lesions are made up of a variety of rare (<1/100000) nonglial neoplasms (Crocetti et al. 2012). Overall survival is influenced by many factors including the tumor cell origin, location, grade, and genetic mutational status. Pretreatment prognosis is usually expressed in the form of percentage survival at x years: For example, 5-year survival is around 50% for patients under 40 years and 60% for childhood and adult tumors growing in eloquent regions of the brain, whereby intrinsic masses are associated with reduced survival. The tumor genetic signature represents a principal determinant of prognosis, which for certain lesions is greater than cell morphology and histological grade. More aggressive tumors often arise in the elderly, in whom comorbidities may limit resectability. Lesion location contributes to the prognosis as this may relate to eloquent function, and the pressure tolerance is less in smaller compartments (e.g., infratentorial versus supratentorial). Research efforts are ongoing worldwide to improve the often limited survival of patients with brain tumors. As such, an increasing need is expected for the development and clinical translation of novel imaging biomarkers to optimize brain tumor characterization and treatment response assessment.

Clinical Presentation

The clinical presentation of brain tumors is variable ranging from absent or minor nonspecific symptoms to fulminant neurological decline. The pattern and severity of symptoms depends predominantly on lesion location, and fast-growing tumors are more likely to cause symptoms or complications such as hydrocephalus (Fig. 1). For patients diagnosed with brain tumors in the emergency setting, one study (Comelli et al. 2017) found the following clinical signs were found to be common: focal neurological deficits (>50%), altered mental status (24.9%), headache (14.6%), seizures (14.1%), secondary trauma (7.8%), and less frequently nausea/vomiting/dizziness (4.4%), but figures may vary for nonacute presentations. Details of typical symptoms are discussed below:

Headache: This is commonly a reflection of raised intracranial pressure, either by direct mass effect of the tumor and/or vasogenic edema, by secondary hemorrhage or blockage of cerebrospinal fluid (CSF) passage. Alternatively, pain can occur due to stretching and distortion of the meninges in the absence of raised pressure. A feature distinct from benign headaches, which should prompt exclusion of a brain tumor, is the gradual evolution of associated symptoms (i.e., focal deficit, seizures, ataxia, and vomiting) or a significant change in a prior headache pattern.

Seizures disorders: For focal seizures, their semiology is dependent on the tumor location and may either remain partial or become generalized. An inverse relationship between tumor grade and occurrence of seizures has been reported, whereby some cortically based low-grade tumors can be associated with seizures in over 90% of cases. Seizures can however not be viewed as a reassuring feature as they may also be the first presentation of an aggressive malignancy.

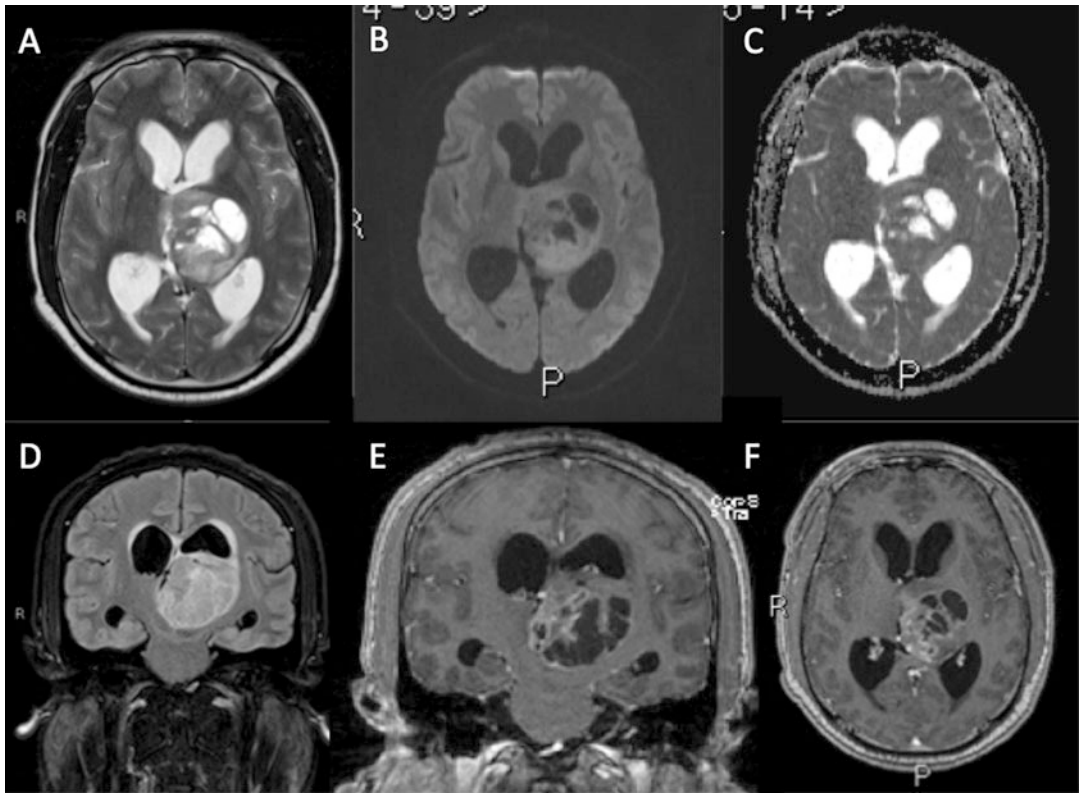

Fig. 1 T2w (**a**), b1000 DWI and ADC map (respectively, **b** and **c**), FLAIR (**d**), and T1w + Gad images (**e**, **f**) in a teenage patient with diffuse midline glioma, H3 K27 M-mutant (WHO grade IV). Rapid growth of this highly malignant tumor has resulted in obstructive hydrocephalus

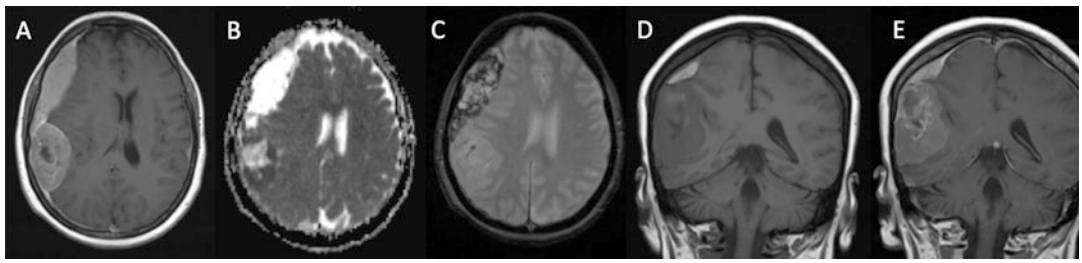

Fig. 2 T1w + Gad (**a**), ADC map (**b**), T2* (**c**), pre- and post-Gad T1w (**d**, **e**) images in a patient with acute cerebral convexity subdural hemorrhage as a complication of adjacent breast cancer metastatic infiltration

Specific Signs

- Focal deficits: These depend on the function of the area where the tumor is located; deficits are more often gradually progressive or less frequently acute, for example in case of intra- or peritumoral hemorrhage (Fig. 2) or vascular changes (e.g., stroke-like presentations or apparent transient ischemic attacks (TIAs). A rare presentation in children and infants is the diencephalic syndrome, with failure to gain weight and to grow as expected, and emaciation due to hypothalamic and thalamic tumors. Affected patients may behave in an alert, happy, and outgoing manner, in contrast to their outward appearance.
- Cognitive, behavioral, and neuropsychiatric symptoms can be associated with specific grey matter areas (e.g., frontal lobe, temporal lobe

dominant parietal lobe, angular gyrus) or brain infiltrating the limbic system or brain networks.
- Cranial nerves and brainstem symptoms: posterior fossa tumors are commonly accompanied by vertigo, dizziness and, if they involve the cerebellopontine angle, they can cause deficits due to compression of cochlear (unilateral hearing loss), trigeminal and/or facial nerves (hypoesthesia numbness, facial weakness, depression of corneal reflex), and the brainstem (Parinaud's syndrome and hydrocephalus). Anterior fossa tumors can present with anosmia without any other symptoms, caused by compression of olfactory nerves.
- Endocrine symptoms: hormonal disturbances (lack or oversecretion of anterior or posterior pituitary, precocious puberty) or visual deficits (e.g., bitemporal quadrantanopia or hemianopia due to optic chiasm compression) can be an effect of pituitary and hypothalamic tumors.

Differential Diagnosis

Nonneoplastic Disease

Lesion morphology often permits an unambiguous distinction between tumor and other entities, but occasionally imaging features overlap on multiple MR imaging sequences. The question whether a mass could be nonneoplastic must form part of the neuroradiological review, more so where patients with a newly identified space occupying process are referred for tissue diagnosis (Fig. 3).

Certain diseases, which exert focal mass effect, are often distinguishable from tumor by their typical pattern, e.g., abscess formation (Fig. 4) or hyperacute ischemic infarction on diffusion MRI. But the diagnosis may no longer be straightforward for subacute ischemia, more so where the symptom onset appears gradual. Depending on the timing and etiology (e.g., venous, subacute arterial, or vasculitis) of onset, ischemia may raise concern for a malignant glioma (Fig. 5). Serial imaging showing spontaneous improvement (decrease in mass effect) or fluctuation of changes can provide a useful clue to a nonneoplastic differential.

Tumor mimics are a diagnostic pitfall especially when the clinical information is incomplete or misleading. Examples of this could include omission of systemic inflammatory signs or undiagnosed immunosuppression (Fig. 6).

On the contrary, patients with a suspected non-neoplastic differential may harbor a brain tumor. For this reason, careful inspection of acute CT imaging is advisable, specifically to distinguish infarction from vasogenic edema (Fig. 7).

A caveat should also be made that interval therapy of tumors may result in spurious improvement, classically in primary central nervous system lymphoma (PCNSL) after steroid administration (Fig. 8), which can delay treatment if histological results remain inconclusive. Incorporating

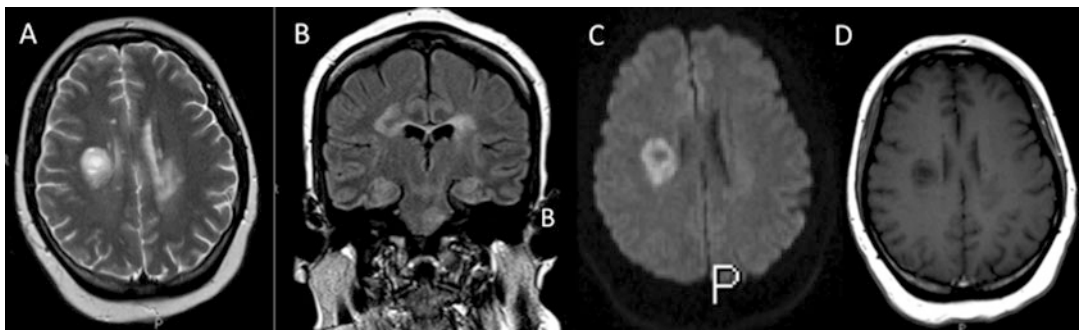

Fig. 3 Tumor mimic: tumefactive demyelination T2w (**a**), T2w-FLAIR (**b**), b1000 DWI (**c**), and T1w + Gad (**d**) images in a young adult female demonstrating a right centrum semiovale mass. On closer inspection, multiple lesions are present in the cerebral white matter and also in the brainstem. A diagnosis of multiple sclerosis was subsequently confirmed

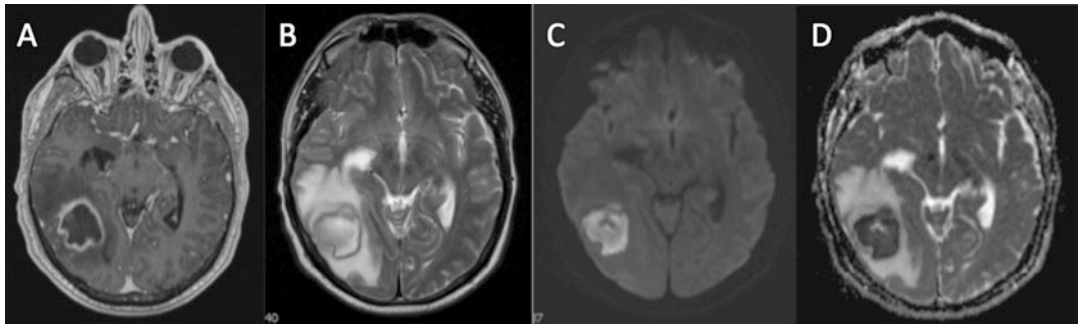

Fig. 4 Tumor mimic: bacterial abscess: T1w + Gad (**a**), T2w (**b**) and diffusion-weighted images (b1000 DWI (**c**), ADC map (**d**)) sequences of a right temporal bacterial abscess characterized by (relatively smooth) rim enhancement, central diffusion restriction, and surrounding vasogenic edema

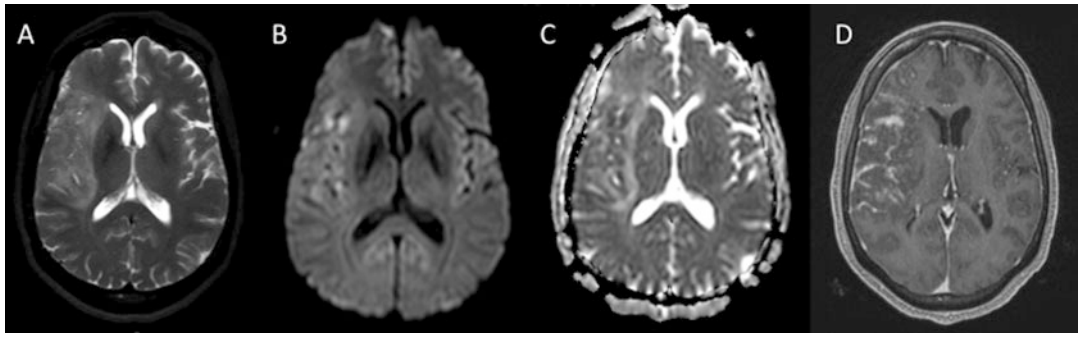

Fig. 5 Tumor mimic: granulomatous vasculitis. T2w (**a**), b1000 DWI (**b**), ADC map (**c**), and T1 + Gad images (**d**) demonstrating a right MCA territory lesion. In this elderly patient, a diagnosis of malignant glioma was considered in the differential due to worsening Gadolinium enhancement and prolonged diffusion restriction. The tissue diagnosis in this case was granulomatous vasculitis

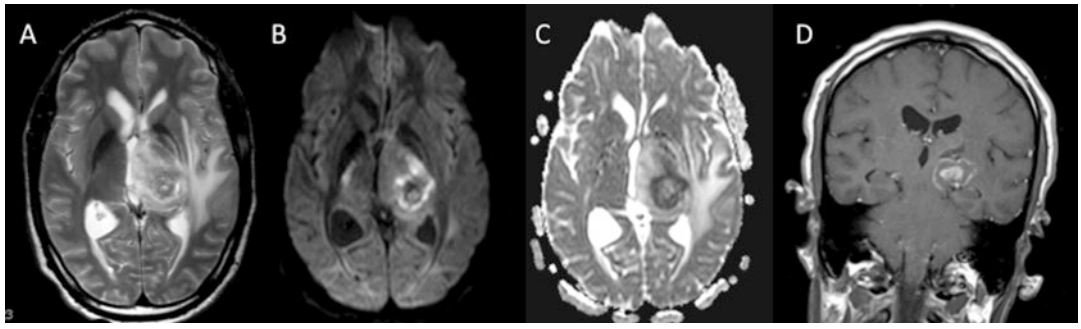

Fig. 6 Tumor mimic: toxoplasmosis. T2w (**a**), b1000 DWI (**b**), ADC map (**c**), and T1 + Gad (**d**) images in a middle-aged male showing a thalamic mass with restricted diffusion and dual rim enhancement ("target sign"). The diagnosis in this previously well individual was toxoplasmosis (acute presentation of an undiagnosed HIV infection)

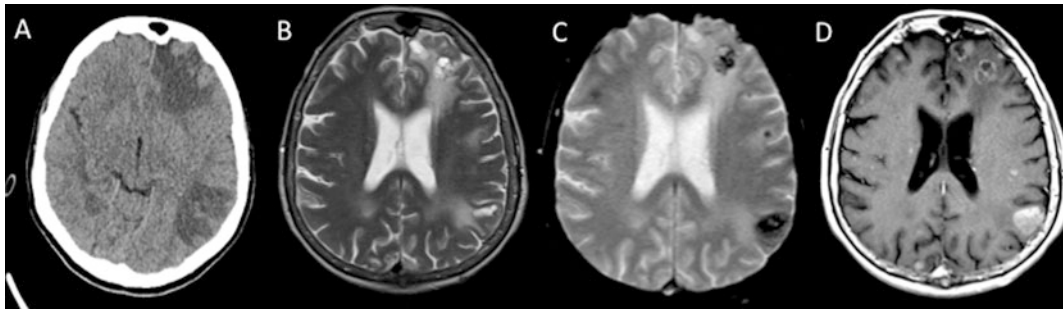

Fig. 7 CT (**a**) images in a patient clinically suspected to have suffered an ischemic stroke. An MRI (T2w, T2*, and T1 + Gad (**b**–**d**)) revealed multiple hemorrhagic deposits with a diagnosis of metastatic lung cancer subsequently established

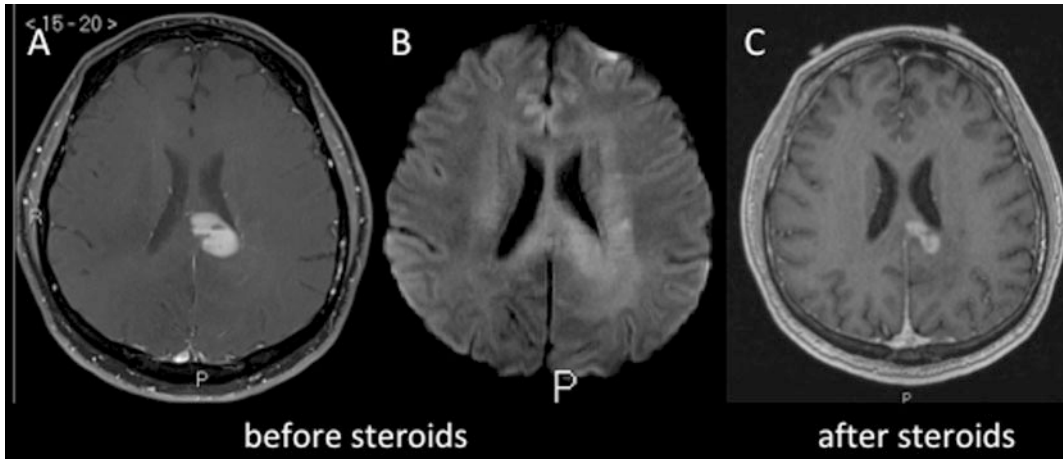

Fig. 8 T1w + Gad and DWI images before (**a**, **b**) versus T1w + Gad images after (**c**) steroid administration in a middle-aged male with suspected primary CNS lymphoma. An inconclusive result was obtained from the first biopsy specimen, with subsequent confirmation of primary CNS lymphoma on repeat biopsy

advanced imaging modalities into clinical practice can aid the identification of tumor mimics. Which modality is most likely to be diagnostic will depend on the particular clinical situation.

Brain Tumors

WHO Classification of CNS Tumors 2016

Brain tumors are not staged according to the familiar TNM (tumor, node, metastasis) system because they rarely spread outside the CNS. Thus, histological and molecular grading are the principal steps of the neuropathological assessment, essential for a realistic prognosis.

The World Health Organisation (WHO) 2016 reclassification (Table 1) underlines that genomic and proteomic analyses, more so than histopathological inspection, are key outcome determinants in CNS tumors. With the discovery of molecular data, the new brain tumor classification has adopted a major diagnostic change to the extent that certain histomorphological groups such oligoastrocytoma, gliomatosis, or primitive neuroectodermal tumor (PNET) are discontinued because they dissolve into different genetic, prognostically more meaningful categories. Other entities are newly commenced, for example,

Table 1 The 2016 World Health Organization classification of tumors of the central nervous system (with permission from Louis et al. 2016)

WHO classification of tumors of the central nervous system	
Diffuse astrocytic and oligodendroglial tumors	
Diffuse astrocytoma, IDH-mutant	9400/3
Gemistocytic astrocytoma, IDH-mutant	9411/3
Diffuse astrocytoma, IDH-wildtype	*9400/3*
Diffuse astrocytoma, NOS	9400/3
Anaplastic astrocytoma, IDH-mutant	9401/3
Anaplastic astrocytoma, IDH-wildtype	*9401/3*
Anaplastic astrocytoma, NOS	9401/3
Glioblastoma, IDH-wildtype	9440/3
Giant cell glioblastoma	9441/3
Gliosarcoma	9442/3
Epithelioid glioblastoma	*9440/3*
Glioblastoma, IDH-mutant	9445/3*
Glioblastoma, NOS	9440/3
Diffuse midline glioma, H3 K27 M-mutant	9385/3*
Oligodendroglioma, IDH-mutant and 1p/19q-codeleted	9450/3
Oligodendroglioma, NOS	9450/3
Anaplastic oligodendroglioma, IDH-mutant and 1p/19q-codeleted	9451/3
Anaplastic oligodendroglioma, NOS	*9451/3*
Oligoastrocytoma, NOS	*9382/3*
Anaplastic oligoastrocytoma, NOS	*9382/3*
Other astrocytic tumors	
Pilocytic astrocytoma	9421/1
Pilomyxoid astrocytoma	9425/3
Subependymal giant cell astrocytoma	9384/1
Pleomorphic xanthoastrocytoma	9424/3
Anaplastic pleomorphic xanthoastrocytoma	9424/3
Ependymal tumors	
Subependymoma	9383/1
Myxopapillary ependymoma	9394/1
Ependymoma	9391/3
Papillary ependymoma	9393/3
Clear cell ependymoma	9391/3
Tanycytic ependymoma	9391/3
Ependymoma, *RELA* fusion-positive	9396/3*
Anaplastic ependymoma	9392/3
Other gliomas	
Chordoid glioma of the third ventricle	9444/1
Angiocentric glioma	9431/1
Astroblastoma	9430/3
Choroid plexus tumors	
Choroid plexus papilloma	9390/0
Atypical choroid plexus papilloma	9390/1
Choroid plexus carcinoma	9390/3
Neuronal and mixed neuronal-glial tumors	
Dysembryoplastic neuroepithelial tumor	9413/0
Gangliocytoma	9492/0
Ganglioglioma	9505/1
Anaplastic ganglioglioma	9505/3
Dysplastic cerebellar gangliocytoma (Lhermitte–Duclos disease)	9493/0
Desmoplastic infantile astrocytoma and ganglioglioma	9412/1
Papillary glioneuronal tumor	9509/1
Rosette-forming glioneuronal tumor	9509/1
Diffuse leptomeningeal glioneuronal tumor	
Central neurocytoma	9506/1
Extraventricular neurocytoma	9506/1
Cerebellar liponeurocytoma	9506/1
Paraganglioma	8693/1
Tumors of the pineal region	
Pineocytoma	9361/1
Pineal parenchymal tumor of intermediate differentiation	9362/3
Pineoblastoma	9362/3
Papillary tumor of the pineal region	9395/3
Embryonal tumors	
Medulloblastomas, genetically defined	
Medulloblastoma, WNT-activated	9475/3*
Medulloblastoma, SHH-activated and *TP53*-mutant	9476/3*
Medulloblastoma, SHH-activated and *TP53*-wildtype	9471/3
Medulloblastoma, non-WNT/non-SHH	9477/3*
Medulloblastoma, group 3	
Medulloblastoma, group 4	
Medulloblastomas, histologically defined	
Medulloblastoma, classic	9470/3
Medulloblastoma, desmoplastic/nodular	9471/3
Medulloblastoma with extensive nodularity	9471/3
Medulloblastoma, large cell/anaplastic	9474/3
Medulloblastoma, NOS	9470/3
Embryonal tumor with multilayered rosettes, C19MC-altered	9478/3*
Embryonal tumor with multilayered rosettes, NOS	*9478/3*
Medulloepithelioma	9501/3
CNS neuroblastoma	9500/3
CNS ganglioneuroblastoma	9490/3
CNS embryonal tumor, NOS	9473/3

(*continued*)

Table 1 (continued)

WHO classification of tumors of the central nervous system	
Atypical teratoid/rhabdoid tumor	9505/3
CNS embryonal tumor with rhabdoid features	*9508/3*
Tumors of the cranial and paraspinal nerves	
Schwannoma	9560/0
Cellular schwannoma	9560/0
Plexiform schwannoma	9560/0

*these new codes were approved by International Agency for Research on Cancer (IARC)/WHO Commitee for the ICD-O (International Classification of Diseases for Oncology).

"diffuse midline glioma, H3 K27M-mutant" (shown in Fig. 1), "multinodular vacuolating glioneuronal tumor" (Fig. 9) (Nunes et al. 2017; Thom et al. 2018) and several pediatric embryonal tumor classes. With this, brain tumor imaging has to face additional challenges at the level of the initial diagnosis, within the context of the WHO classification and in treatment response monitoring.

Narrowing the Tumor Differential

Once the possibility of nonneoplastic disease has been dismissed, generating a list of tumor differential diagnoses should follow as the next step. The following section suggests a diagnostic approach to review the combination of patient age, clinical features, and lesion location in order to reduce the number of possible diagnoses (Osborn et al. 2016; Clarke et al. 2016).

Influence of Age

- Tumors in children other than newborns are commonly infratentorial, whereas primary neoplasms in adults are mostly supratentorial.
- Common neoplasms in children are astrocytoma, ependymoma, and embryonal tumors including medulloblastoma.
- The more frequent early to middle life tumors are gliomas, meningiomas, and pituitary adenomas.
- In older adults, glioblastoma and metastases are more common, and there is also an increasing incidence of primary CNS lymphoma.

Symptom Evolution

The clinical presentation of a brain tumor depends on location, rate of growth, and pathology. High-grade tumors, intra−/periventricular and posterior fossa mass lesions are more likely to produce a focal deficit and raised intracranial pressure because of the rapid growth within a confined compartment and/or hydrocephalus. By contrast, slowly growing, cortically based neoplasms (such as DNET, ganglioglioma, oligodendrogliomas) are more indolent and present frequently with a seizure disorder. However, it must be noted that highly aggressive lesions, including glioblastoma, may also present with seizures. Widely infiltrating tumors such as astrocytic tumors with a gliomatosis cerebri growth pattern can also present with cognitive and neuropsychiatric symptoms. At an early stage, malignancy can be asymptomatic or appear innocuous on imaging. No pathognomonic symptomatology exists for any brain tumor type.

In addition, certain tumors, in particularly small cell lung metastases and hematological malignancies, may present with paraneoplastic limbic encephalitis, which is typically associated with memory and cognitive problems and usually diagnosed by T2/FLAIR hyperintense signal in the hippocampi that may be symmetrical or asymmetrical (Fig. 10).

Lesion Location

Cortically based tumors

- DNET
- Ganglioglioma
- Oligodendroglioma
- Pleomorphic XanthoAstrocytoma (PXA)

Intraventricular tumors

- Ependymoma, subependymoma
- Central neurocytoma

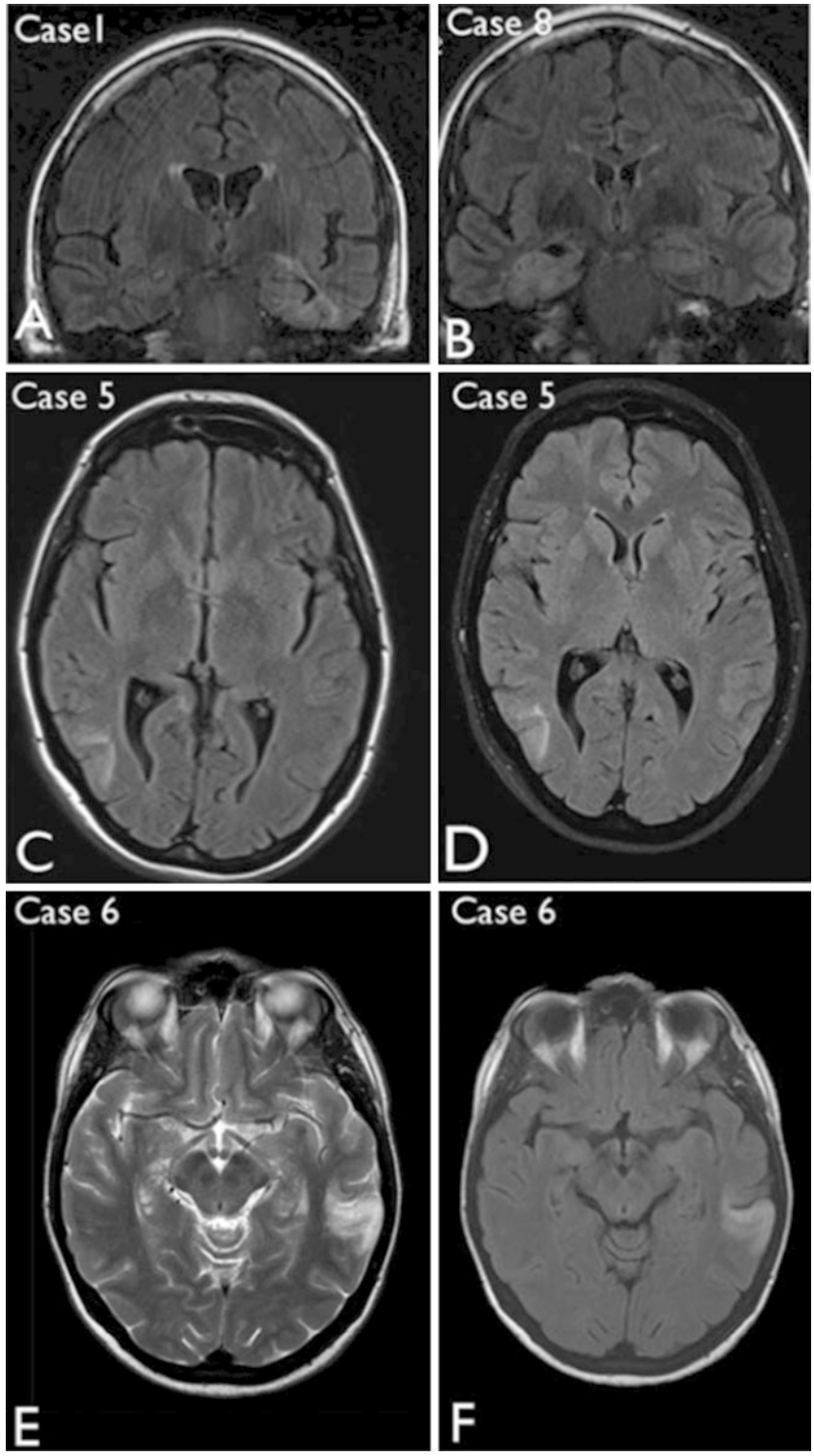

Fig. 9 Multinodular vacuolating glioneural tumor, several case examples on FLAIR (**a**–**d**, **f**) and T2 w (**e**) imaging with permission from Thom et al. (2018)

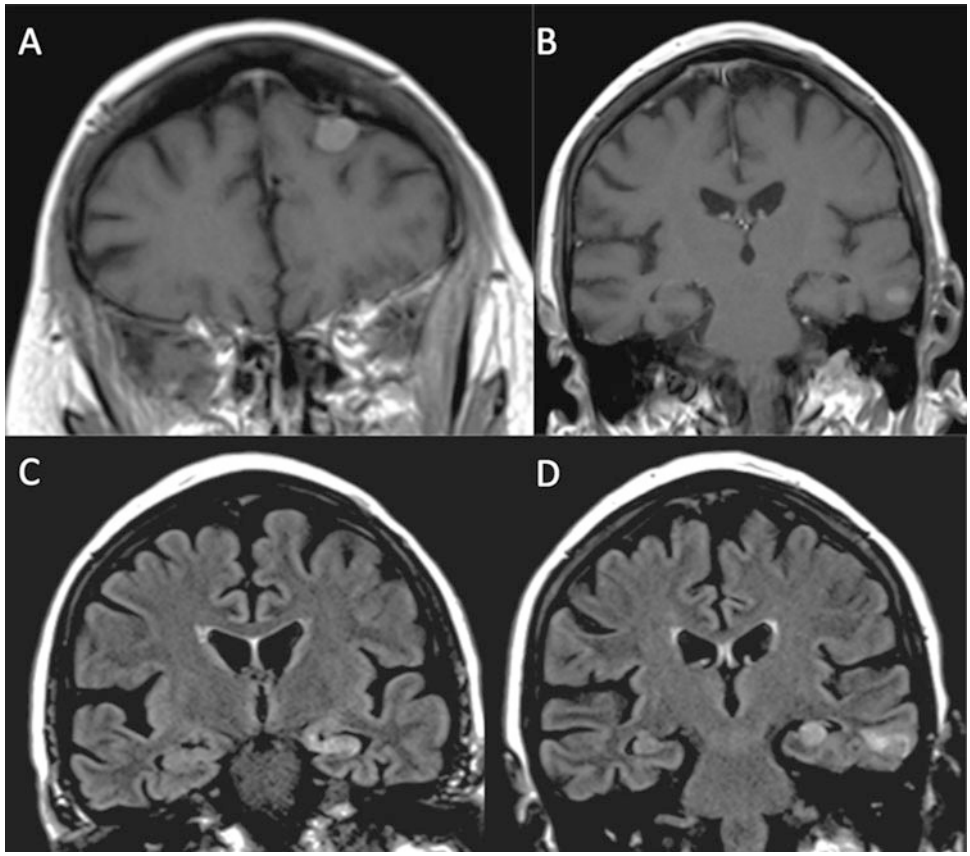

Fig. 10 Dual disease: T1w + Gad (**a**, **b**) and FLAIR (**c**, **d**) images in a patient with metastatic small cell lung cancer. In this case, metastatic deposits coexisted with paraneoplastic limbic encephalitis (left mesial temporal FLAIR signal hyperintensity)

- Choroid plexus papilloma/carcinoma
- Pilocytic astrocytoma in third ventricle and cerebellum
- Meningeoma

Pineal region tumors

- Pineal parenchymal tumors (pineocytoma/blastoma)
- Germ cell tumors
- "Other" tumors/masses: Nonneoplastic pineal cyst, Astrocytoma (rare), Meningioma (tentorial dural attachment)

Meningeal tumors and mimics

- Meningioma
- Metastasis, lymphoma
- Inflammatory pseudotumor
- Infection (e.g., tuberculosis)
- Extramedullary hematopoiesis

Extracranial neoplasms with intracranial extension

- Chordoma
- Paraganglioma
- Carcinomas (e.g., nasopharyngeal squamous cell), sarcomas (rhabdomyosarcoma)

Cystic and nodule appearances

- Pilocytic astrocytoma
- Craniopharyngioma
- Ganglioglioma
- Hemangioblastoma

Imaging Work-Up

Tremendous efforts are put into a better understanding of the pathophysiology of brain tumors. The central aim of conventional and advanced imaging techniques is to gather information to guide therapy and to monitor response, which includes identification of complications or need for additional treatment at the earliest possible time point.

Anatomical MRI provides the first step to identify the lesion location, to approximate its extent, and to generate a list of differential diagnoses. Depending on the clinical situation, standard MR imaging may suffice, but commonly advanced sequences offer additional diagnostic value. Imaging can be further integrated by merging imaging data sets with genetic and features (radiomics), with or without machine learning strategies. For some of the newer tools, translational research is ongoing and further work will be required to establish robust, multicenter applicable scanning, and postprocessing protocols for clinical care. In the following section, information is provided on the role of different imaging modalities, which may support brain tumor assessment. This is followed by a suggestion for a standard imaging protocol, which may be further supplemented by advanced techniques on an individual case basis.

Imaging Modalities in Neuro-oncology

Computed Tomography

Despite its limited contrast resolution, it is acknowledged that CT has an important role in acute care to identify hemorrhage, critical mass effect, or hydrocephalus requiring emergency neurosurgical intervention. In addition, CT is useful in the assessment of extra-axial tumors to assess the integrity of the skull vault and hyperostotic bone reaction.

Anatomical MRI

Anatomical MRI represents the basic standard of care imaging method in neuro-oncology. Current best practice recommendations for a standardized brain tumor MRI protocol are to include volumetric (3D) T1-weighted images (T1w) before and after Gadolinium contrast injection, 2D or 3D axial fluid-attenuated inversion recovery (FLAIR), 2D axial diffusion-weighted imaging (DWI), and axial T2-weighted images (T2w) using a 1.5 or 3 tesla MR system. The use of volumetric imaging has been shown to increase small lesion visibility and can support volumetric tumor measurements. It is considered preferable to acquire T2w after gadolinium in order to standardize the minimal time between the injection and acquisition of postcontrast T1-weighted images. Imaging parameters (such as contrast dose and timing) should be maintained consistently to maximize serial comparability, as brain tumor patients generally require long-term follow-up.

Physiological MR Imaging

Methods that can visualize and quantify pathophysiological, cellular, and/or metabolic processes in tumors are becoming increasingly used in clinical practice. At the initial diagnosis, advanced MRI aims to predict malignant potential and plan surgical biopsy/resection, whereas in the post therapeutic stage these techniques can help to distinguish viable tumor from therapy effects, both of which may appear similar on conventional Gadolinium enhanced MRI due to blood-brain-barrier breakdown.

Recently, global initiatives have formed to pursue the standardized development of physiological imaging biomarkers, which include the Quantitative Biomarkers Alliance (QUIBA) and the American College of Radiology Imaging Network (ACRIN). Table 2 provides an overview of typical brain tumor and nonneoplastic lesion appearances on physiological MR sequences.

Diffusion-Weighted MRI (DWI)

Diffusion image signal is influenced by cell density and matrix composition; therefore, cellular brain tumors tend to exhibit low diffusivity. Three-

Table 2 Overview of typical diffusion, perfusion, and spectroscopy features of intracranial mass lesions. Information is approximated for guidance; please note that quantitative values can vary according to imaging parameters, postprocessing, and measuring technique

Intracranial mass lesions	DWI (ADC)	DSC perfusion (rCBV)	1H MRS
Neoplasm			
High grade glioma	Often heterogenous, ↓ in solid tumor, but may exhibit ADC similar to normal brain without true restriction	↑ in solid tumor and sometimes in the peritumoral zone	↓ NAA and myo-inositol, ↑choline, ↑ lactate/lipid peak (1.33 ppm) ↑ Glycine
Astrocytoma, IDH wild-type	Variably ↓	Variably ↑	Variably ↓ NAA & myo-inositol, ↑choline, +/− ↑ lactate/lipid peak (1.33 ppm)
Low grade glioma 1. Oligodendroglioma ($IDH_{mut}1p91q_{del}$) 2. Astrocytoma (IDH_{mut})	1. Intermediate 2. ↑	1. Intermediate to ↑ 2. Low, unless anaplastic transformation	1. ↑ Cho, ↓ NAA, MI/Cr ratio ↑ 2. ↑ Cho & MI/Cr ratio, ↓ NAA
Lymphoma	↓, may exhibit true restriction (ADC values < normal brain)	↓ to intermediate rCBV	↓ NAA, ↑ Cho, ↑ lipid/lactate peaks reported
Metastases	Variably ↓-↑, depending on primary origin	↑ in solid tumor ↓ in the peritumoral zone	Spectra resembling tumor
Central neurocytoma	↓	↓	↑ Cho peak &Cho/Cr ratios typical, notable peak at 3.55 ppm (glycine), inverted alanine peak at 1.5, NAA presence
Nonneoplastic masses			
Tumefactive demyelination	↓ peripherally, ↑ centrally	↓	↑choline, lactate, glutamate/glutamine (Glx) at 2.4 ppm
Bacterial abscess	↓ centrally	↓	Lipid and lactate levels of 1.3 ppm and amino acid levels of 0.9 ppm with or without the presence of succinate, acetate, alanine, and glycine
TB abscess	↓↑ centrally	↓	Only lipid and lactate levels of 1.3 ppm
Toxoplasmosis	↑ in abscess, ↓in abscess wall	↓centrally and in the perilesional edema	↑ lactate and lipids, ↓Cho; variable ↓ Cr & NAA
Epidermoid cyst	↓	↓	Lactate occasionally
Arachnoid cyst	↑	↓	Minimal lactate occasionally
Perivascular space	↑	↓	No abnormalities (rarely ↑ lactate levels reported)
Subacute hematoma	↓ centrally	Susceptibility artifacts	Susceptibility artifacts
Chronic hematoma	↑	Susceptibility artifacts	Susceptibility artifacts

directional DWI should form part of clinical brain tumor imaging and may be performed with two or three b values, typically b0, (+/−b500) and b1000 mm/s^2. From this, the ADC map is calculated through mathematical subtraction of T2 effects, which permits quantitative diffusion measurement. Note that low diffusivity does not equal high malignant potential but requires interpretation in context with lesion morphology, as this can be present in benign tumors (e.g., WHO I meningioma) and some noncancerous lesions (e.g., epidermoid cyst, Fig. 11). Malignant gliomas may not necessarily show diffusion restriction, instead they may appear similar to surrounding brain on ADC maps. Diffusion-weighted imaging is the optimal modality to identify cytotoxic edema and can aid the distinction of purulent infection from brain tumor.

Diffusion tensor imaging (DTI) is used to gain information about the directionality of water diffusion by examining six or more diffusion directions. Within tissues, water typically moves more easily into some directions than others, for example, in the brain water preferentially diffuses along rather than perpendicular to tightly bound axons. This quantifiable phenomenon is termed fractional anisotropy (FA). DTI data can be reconstructed to visualize peritumoral white matter tracts (tractography, Fig. 12) in color for surgical planning and is commonly integrated into surgical navigation devices. Other more complex DWI techniques, based on the assumption that water diffusion has a non-Gaussian distribution, include compartmental diffusion modeling and kurtosis imaging, which can be used

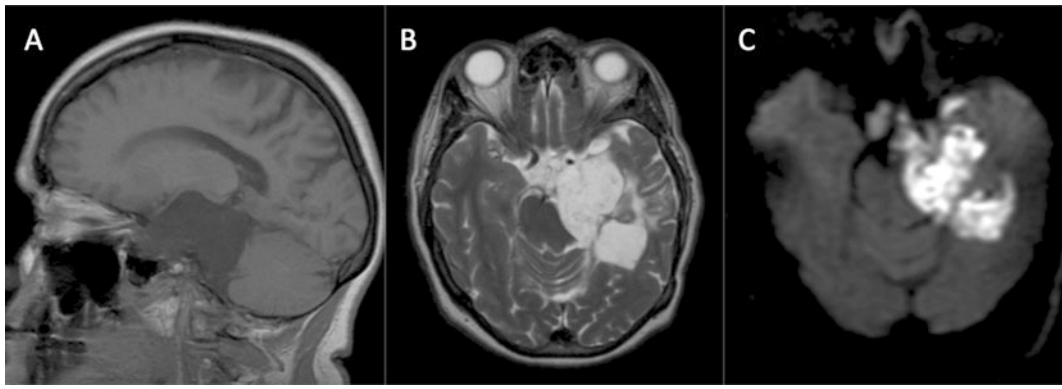

Fig. 11 Epidermoid cyst. T1w (**a**), T2w (**b**), and b1000 DWI (**c**) images highlighting typical features of an extra-axial, in particular diffusion restriction (ADC map not provided)

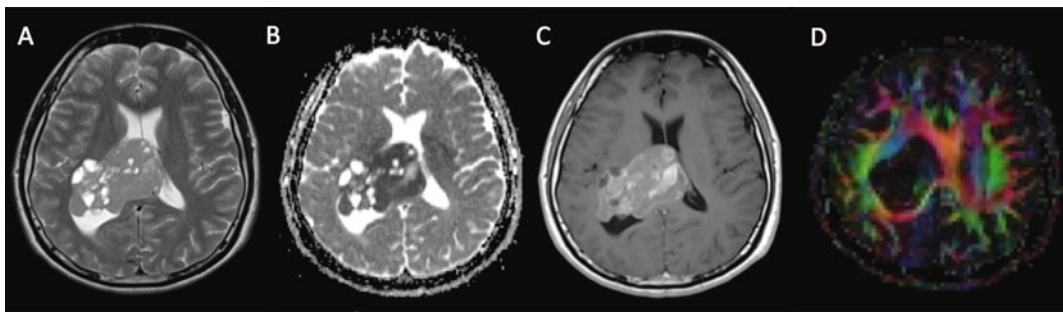

Fig. 12 T2w (**a**), ADC map (**b**) and T1w + Gad images (**c**) in a patient with central neurocytoma, who subsequently underwent surgical resection. Additional diagnostic information was gained from the DTI tractography (**d**), which reveals distortion of white matter tracts around the mass

to calculate tissue microstructural properties such as diffusion heterogeneity.

Perfusion-Weighted MRI (PWI)

Certain types of primary neoplasms and metastases exhibit greater vascularity than surrounding brain, which can be exploited in differential diagnosis, for biopsy targeting and to identify disease recurrence. In high grade gliomas, elevation of certain perfusion parameters such as the relative cerebral blood volume (rCBV) and relative cerebral blood flow (rCBF) reflects neovascularity, but this has limited specificity as low grade oligodendrogliomas may share similar appearances. PWI requires interpretation in conjunction with structural imaging, as rCBV and rCBF may be high in more benign masses (e.g., meningioma, hemangioblastoma) or relatively low in aggressive tumors such as PCNSL. PWI can improve the distinction of adjuvant therapy effects (Fig. 13) from malignant tumor recurrence, as perfusion tends to be more markedly elevated in viable (neovascular) tumor.

Several MR perfusion methods exist: Dynamic Susceptibility Contrast (DSC) imaging, which is currently the most commonly used technique, and Dynamic Contrast-enhanced (DCE) imaging require both an intravenous injection of a gadolinium-based contrast medium, whereas arterial spin labeling (ASL) perfusion imaging does not.

- DSC shows a transient vascular signal reduction on T2*-weighted images during the first pass of a gadolinium bolus injection due to paramagnetic effects. A volume of T2* images is repeatedly acquired at rapid (1–2 s) intervals before and during the contrast injection taking

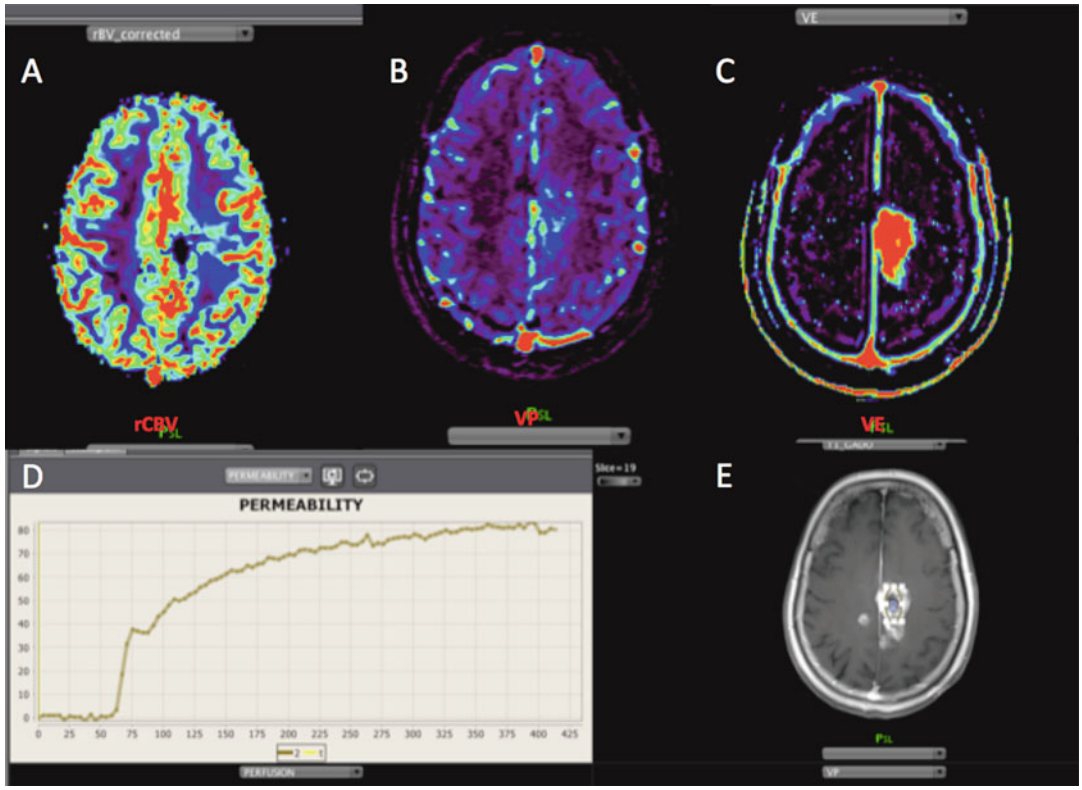

Fig. 13 DSC-derived relative cerebral blood volume map (**a**), DCE-derived Vp (**b**), Ve (**c**), time-signal-intensity curve (**d**) and corresponding T1w + Gad image (**e**) of a recurrent enhancing mass in a previous radiotherapy recipient. Blood volume is mildly raised, but Ve signal is much greater than Vp, and there is delayed progressive contrast wash-in in keeping with predominating radionecrosis

approximately 1–2 min in total. For tumor imaging, the rCBV is the most used and best validated DSC parameter. Acquisition, post-processing, and observer factors may affect perfusion measurement; therefore, a standardized imaging protocol with consistent technical parameters is recommended, which may include a preload bolus to minimize T1 leakage effects in the presence of a disrupted blood brain barrier (Welker et al. 2015). DSC imaging may be severely hampered or nondiagnostic in the presence of marked susceptibility artifacts from intratumoral hemorrhage or after surgical intervention.

- Dynamic contrast-enhanced MRI (DCE) measures the increase of signal intensity on T1-weighted images from baseline after gadolinium administration over a certain time period (typically around 5–7 min). The time–signal intensity curve depends on tissue perfusion and vascular permeability and the concentration of gadolinium in the intravascular as well as extravascular-extracellular space. DCE data can be analyzed by using the shape of the time-signal intensity curve to identify rapidly enhancing hyperperfused tumor or slow leakage of contrast medium into the extravascular extracellular space. Mathematical modeling (e.g., the Tofts model and extended Tofts Model) can provide quantitative measurements such as the transfer coefficient $K^{trans.}$ which depends on endothelial permeability, vascular surface area, and blood flow within the tissue of interest. Further parameters of interest are plasma volume (Vp), which has been shown to correlate with DSC derived rCBV, and the volume of the extravascular extracellular space (Ve). Contrary to DSC, DCE is not compromised by intralesional susceptibility artifacts, which can be significant following surgery, and has the advantage of increased spatial resolution.
- ASL uses magnetically labeled blood as endogenous tracer to assess tissue blood flow. This newer technique requires no contrast injection and is unaffected by intra or perilesional susceptibility effects. ASL is increasingly used and is particularly suitable for the pediatric population and patients in whom gadolinium injections should be avoided. In the light of recent concerns about gadolinium deposition in the brain, ASL likely attract growing interest.

MR Spectroscopy (MRS)

Functional information about brain masses can be gained from examining the tissue metabolite distribution. Spectroscopy can be performed in form of a single voxel analysis, which is technically easier to achieve but assumes the average values of metabolites within the measured area. Good quality spectra are more complex to achieve using multivoxel spectroscopy, but this has the advantage of being able to identify spatial variations.

MRS is becoming increasingly available in clinical practice; in neuro-oncology it has a recognized role in the distinction of tumor from non-neoplastic conditions, in cases where this is not achieved by other modalities. It can potentially support surgical planning, e.g., biopsy guidance to a metabolic hotspot. A recent meta-analysis, of MRS in gliomas suggested that it may aid the distinction of residual or recurrent tumor from early therapy related changes.

On spectroscopy, tumors are characterized by elevation of choline (Cho) and may feature a decrease in *N*-acetyl aspartate (NAA), a neuron-specific marker and creatine (Cr). Depending on tumor type, lactate or lipids can be present. The rise in Cho occurs due to accelerated synthesis and destruction of cell membranes in growing tissues, which is amplified in areas of high mitotic activity. Lactate accumulation a result of nonoxidative glycolysis (Warburg effect), which generates and perpetuates a tissue milieu conducive to angiogenesis and invasion in malignancy (Fig. 14).

It should be noted that MRS spectra are influenced by the choice of echo time (TE): using a short TE (20–40 ms) smaller metabolites such as *myo*-inositol, glutamate/glutamine and lipids are better demonstrated at the expense of a less stable baseline. Intermediate (135–144 ms) TE allows for a less distorted baseline with improved NAA and Cho quantification with lactate appearing (inconsistently) inverted from the baseline. Long

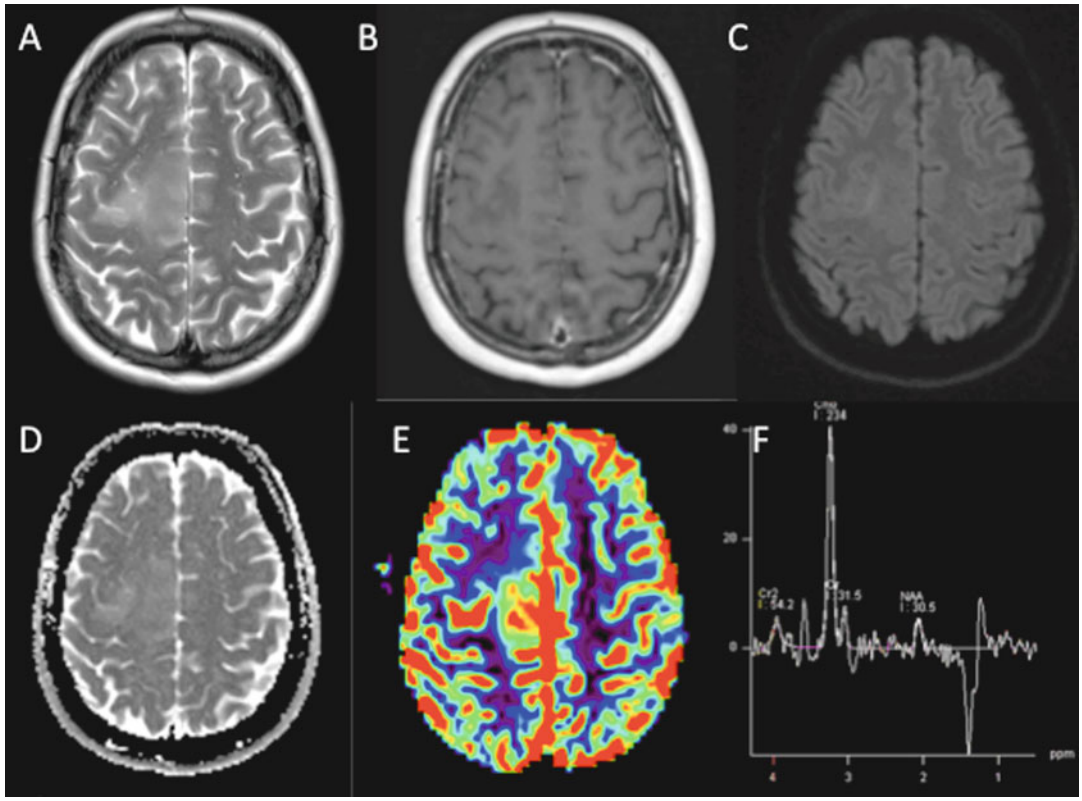

Fig. 14 Value of advanced imaging for the identification of malignant glioma: T2w (**a**) and T1 + Gad images (**b**) demonstrate a non-Gadolinium-enhancing mass. DWI and ADC map (**c**, **d**), DSC perfusion (**e**) and MRS (**f**) reveal low tumor diffusivity (similar to surrounding brain parenchyma), elevated blood volume, and high Choline/NAA ratio in the presence of lactate. The diagnosis in this case was IDH wild-type astrocytoma WHO grade III

(270–288 ms) echo times tend to be less widely used for brain tumor imaging.

Functional MRI (fMRI)

fMRI utilizes blood oxygen level-dependent (BOLD) image signal to depict the transient activation of brain regions as a reflection of neuronal activity. When using fMRI for brain tumor imaging, certain pitfalls exist for example that that BOLD signal may be enhanced by tissue neovascularity and be reduced in the presence of blood products. The most commonly used fMRI technique is task-based, usually in the context of surgical planning to maximize safe resection. Suitable task paradigms depend on the site of planned intervention and can include motor, language and speech production tasks, and/or memory activation. fMRI is most commonly applied for presurgical language lateralization. Alternatively, it can be used to demonstrate cortical eloquent (e.g., motor) functions, specifically whether displacement or functional reorganization has occurred. fMRI is commonly combined with diffusion tractography to depict white matter tracts in the vicinity of a planned resection (Fig. 15).

Positron-Emission Tomography (PET)

In PET imaging, a radioactive substance which accumulates within tumor cells is used to visualize tissue metabolic activity. For brain imaging, the most widely used PET tracer fluorodeoxyglucose [^{18}F] (FDG) typically provides limited tumor to background contrast due to the high

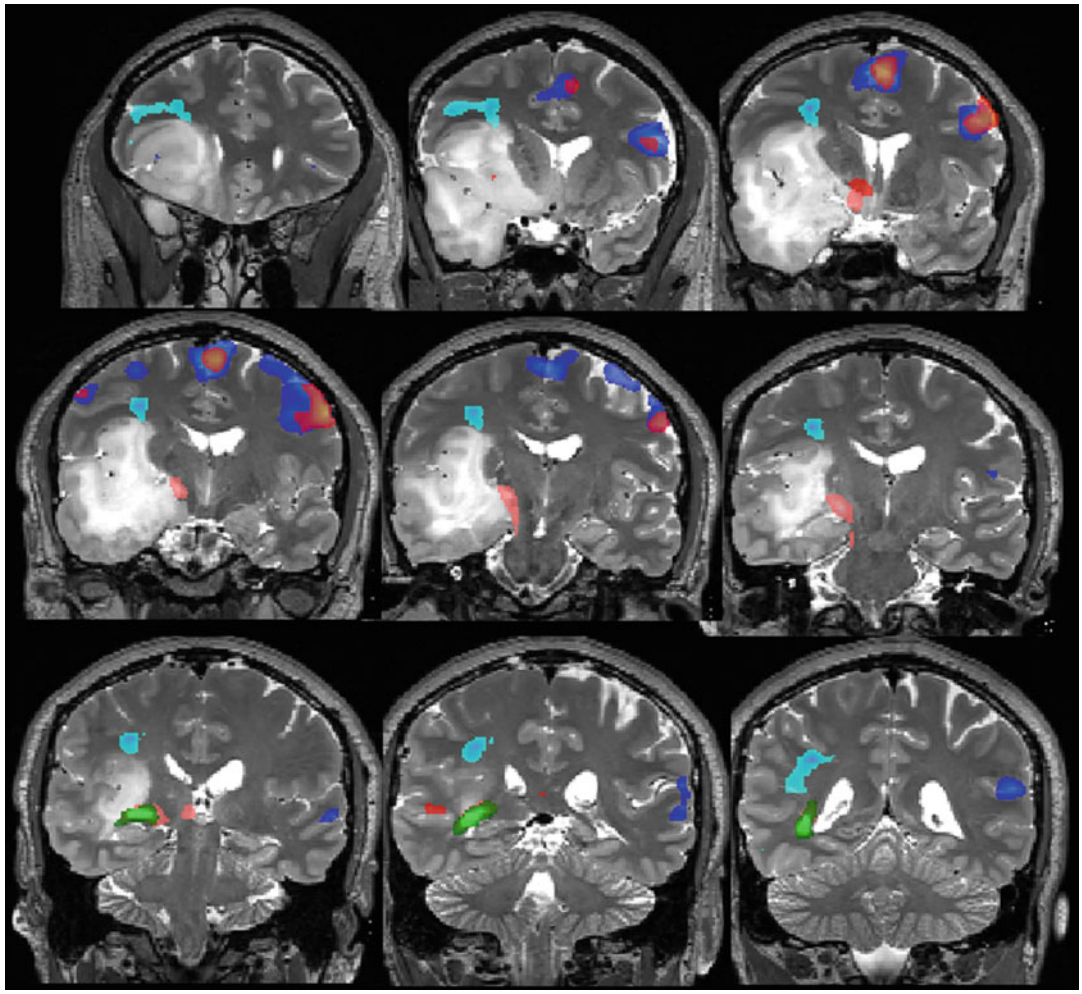

Fig. 15 Coronal T2w images showing a tumor centered on the right temporal lobe. The fused fRMI (dark blue = verb generation, dark red = verbal fluency) sequences indicate left dominance for language. Also shown are the right arcuate fasciculus (light blue) and right optic radiation (green from lateral geniculate nucleus -LGN- to calcarine and light red from calcarine to LGN). (Courtesy of Dr. L. Mancini, London)

physiological glucose uptake of brain cells. Potentially superior alternatives for brain tumor imaging include amino acid analogues such as [^{11}C] methionine (MET), [^{18}F] fluoroethyl-L-tyrosine (FET), and [^{18}F]dehydroxyphenylalanine (FDOPA) to assess protein metabolism and Choline based tracers ([^{11}C]choline (CHO) or [^{18}F] choline), which may give information on tissue membrane turnover. 68Ga-DOTATOC is useful to identify neoplasms with somatostatin receptors and thereby may aid the diagnosis of meningioma. For short half-life tracers, an onsite cyclotron facility is required. In selected cases, PET may contribute to the characterization of newly identified and treated brain tumors, although its use is supported by limited data. Nevertheless, PET may have a role in brain tumor imaging for problem solving, where standard MRI results are indeterminate (Verburg et al. 2017; Fig. 16).

Novel Techniques

Chemical Exchange Saturation Transfer

A number of additional imaging techniques are being trialed in research for brain tumor imaging, with the main focus on glioma. Worth mentioning

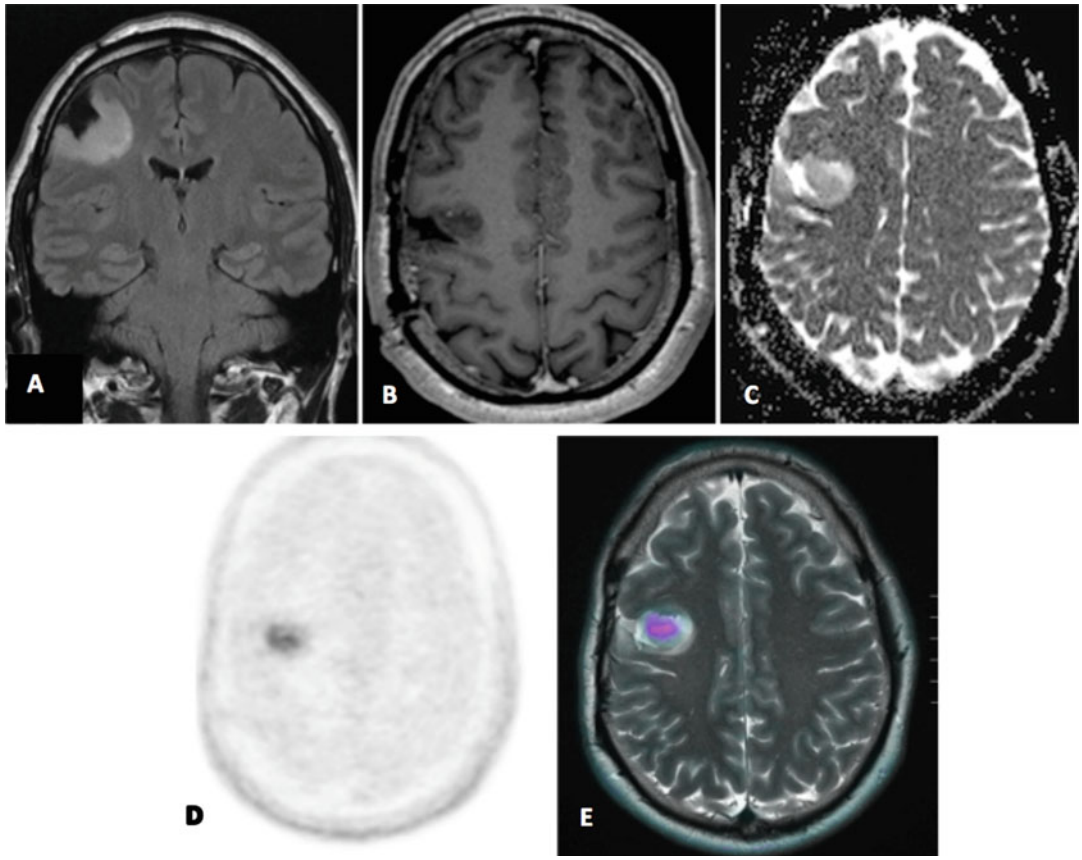

Fig. 16 Coronal T2W FLAIR (**a**), axial postcontrast T1WI (**b**), axial ADC map (**c**), axial ^{18}F DOPA PET (**d**), and axial fused ^{18}F DOPA PET/MR (**e**) demonstrating a nonenhancing area in the right frontal lobe in a patient previously operated for a high-grade glioma. As indicated by increased ^{18}F DOPA tracer uptake, recurrent tumor was present, which was confirmed at surgical resection 2 weeks later (Courtesy of Dr. Francesco Fraioli, London)

among these is Chemical Exchange Saturation Transfer (CEST) imaging, a new contrast mechanism for obtaining metabolic functional information in cancer. Endogenous CEST contrast can be demonstrated in the form of amide proton transfer (APT) as a pH dependent measure of protein turnover. To generate CEST signal, a selective radiofrequency pulse is used to "saturate" exchangeable solute (e.g., amide) protons. The saturation becomes transferred onto surrounding water molecules through chemical exchange and/or dipolar interactions such that the water signal diminishes, which can be exploited to generate images. CEST has a potential to identify malignant glioma metabolism, which could be useful in primary diagnosis and/or follow up (Fig. 17). Whether it has a role in other types of brain tumors is yet to be confirmed.

Texture Analysis and Machine Learning

The field of computational imaging analysis is rapidly expanding with numerous software applications being trialed in research, ranging from histogram analysis to complex artificial intelligence models. Such techniques may be valuable for the characterization of brain tumors, specifically to provide correlation with tumor genetics (radiogenomics), for treated lesions, and to predict survival based on anatomical and/or advanced imaging features.

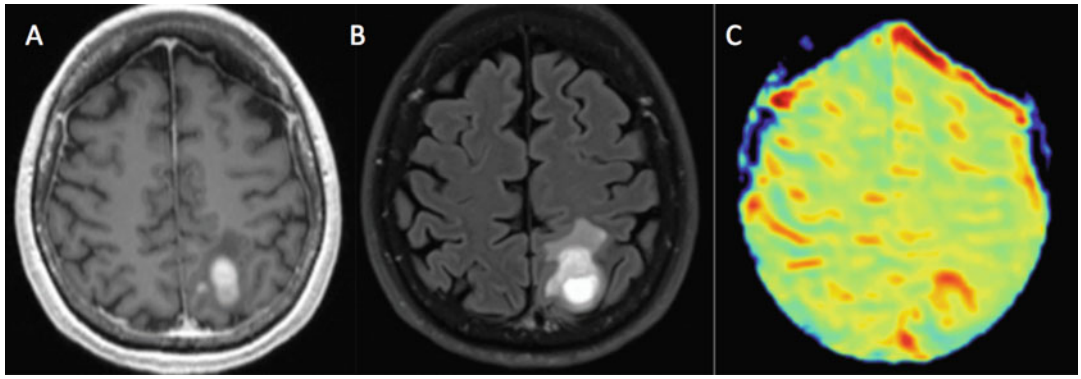

Fig. 17 Postgadolinium T1w (**a**), FLAIR (**b**) and APT-CEST (**c**) imaging in a patient with WHO III astrocytoma. Increased APT signal appears confined to the tumor periphery, suspected to reflect greater focal metabolic turnover, compared to the contrast enhancing lesion center, which shows features of developing necrosis on FLAIR (Courtesy of Prof Pia Sundgren, Lund)

Applications of Physiological Imaging

- Presurgical tumor characterization (prediction of probable origin, WHO grade +/− molecular type)
- Biopsy targeting
- Monitoring response to treatment (includes identification of therapy side effects)

Suggested Imaging Protocol

As essential anatomical sequences, T1w before and after contrast (if possible as a 3D volumetric sequence), DWI, T2w-FLAIR, and T2w sequences are recommended. Table 3 lists three possible options for a brain tumor imaging protocol, whereby option (a) represents the minimum standard and options (b, c) include perfusion.

Additional Sequences

- T2* or SWI: either to identify intratumoral susceptibility signal (ITSS) that may correspond to hemorrhage, calcification, and tumor neovascularity or to visualize biopsy tracts and radiation induced cerebral microbleeds.
- Thin-section and/or small field of view sequences: to examine small structures, e.g. pituitary or pineal gland
- MRS: to distinguish nonneoplastic conditions, tumor characterization, or follow-up when combined with other techniques
- fMRI, DTI: for surgical planning

Sample Case and Report

Case 1

Clinical details: 29-year-old male, originally from Yemen, previously received treatment for hydatid heart disease, presenting with recent onset headaches and seizures (Fig. 18).

Sample Case 1 Report

Technique: Axial T2w, coronal FLAIR, axial DWI/ADC (ADC map not shown), and coronal post contrast T1w images.

Findings: The MR imaging demonstrates a mass centered on the right insula, temporal lobe, and capsular white matter. The lesion exhibits a multicystic appearance with thin peripheral rim enhancement in some parts. Mild mass effect is present with partial effacement of the ipsilateral ventricle, but no midline shift or features of brain herniation. A few additional punctate foci of signal alteration in the left cerebral hemisphere are nonspecific. No further intracranial mass lesion is shown.

Interpretation: In the clinical context, the cystic lesion morphology is concerning for intracranial parasitic dissemination, rather than tumor.

Histological diagnosis: Hydatid disease of the brain.

Table 3 Possible options for a glioma imaging protocol, which could be translated to other brain tumor types. (With permission from Thust et al. 2018). Option (**a**) is based on the European Organisation for Research and Treatment of Cancer and United States National Brain Tumor Society (EORTC-NBTS) imaging protocol (for vendor specific details, please see Ellingson et al. 2015), whereas options (**b**) and (**c**) include perfusion

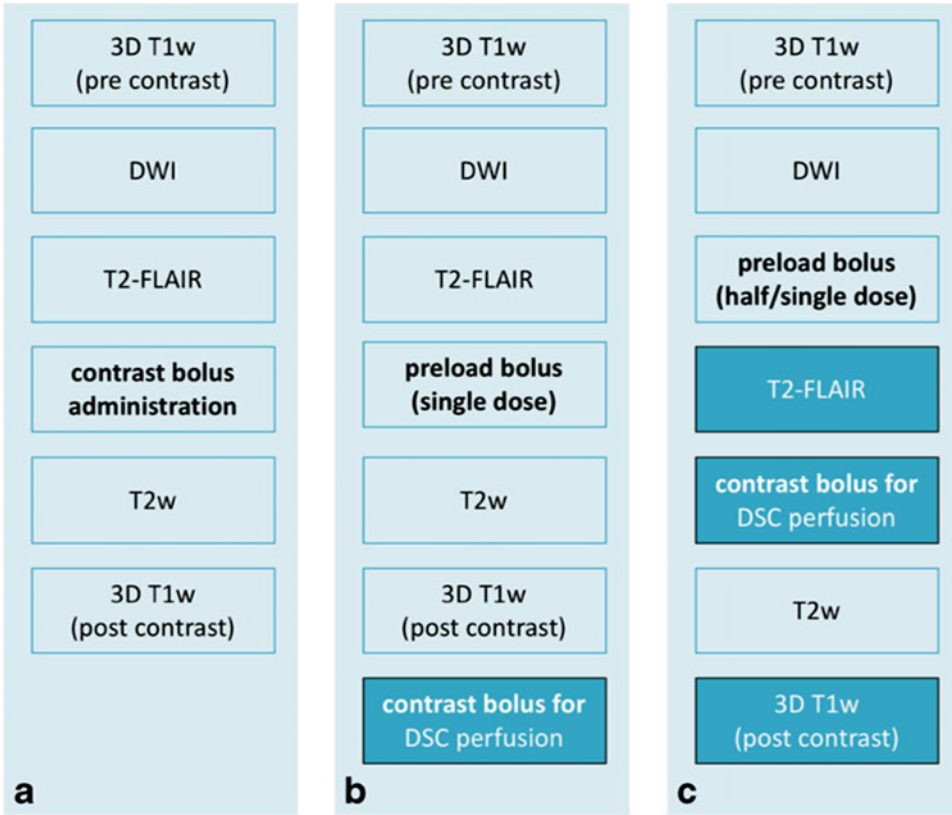

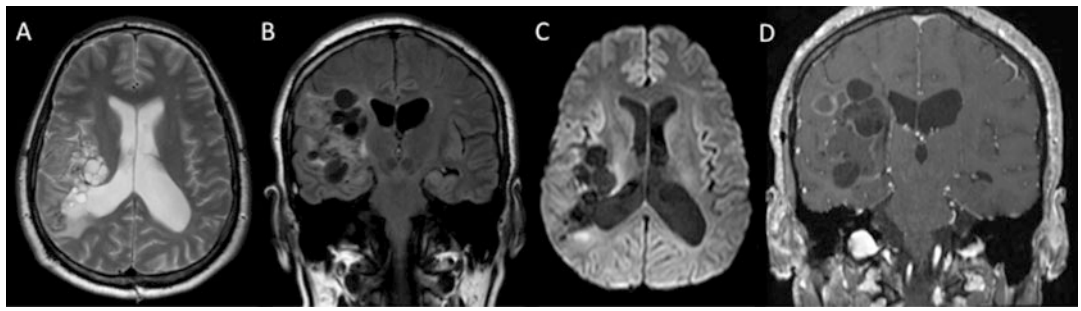

Fig. 18 T2w (**a**), FLAIR (**b**), b1000 DWI (**c**), and post-Gad T1w (**d**) images in sample case 1

Sample Case 2

Clinical details: 50-year-old male, previously well, suffering from recent onset headaches and intermittent poor coordination (Fig. 19).

Sample Case 2 Report

Technique: Axial T2w, ADC map, axial post-Gad T1w images, and DSC perfusion derived rCBV map.

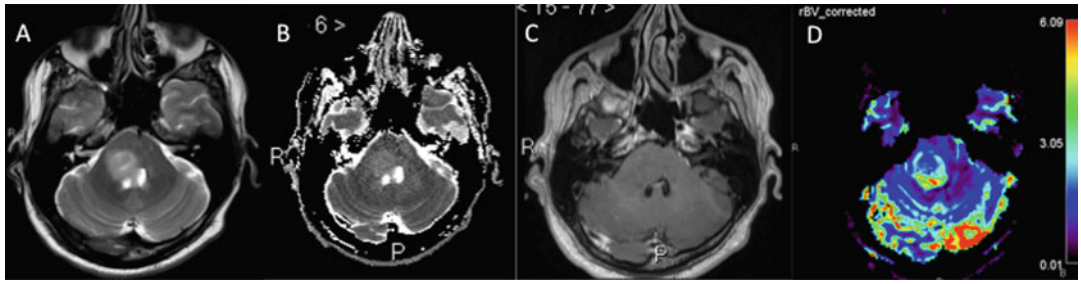

Fig. 19 T2w (**a**), ADC map (**b**), post-Gad T1w images and DSC perfusion derived rCBV map in sample case 2

Findings: The imaging demonstrates a moderately circumscript lesion of mixed T2 signal at the dorsolateral aspect of the right side of the pons. The mass is nonenhancing and displays ADC values similar to surrounding brain parenchyma and increased perfusion (rCBV in the region of 4, compared to normal white matter). There is beginning effacement of the fourth ventricle, but no hydrocephalus at present. The intracranial appearances elsewhere are normal.

Interpretation: Solitary brain stem mass, possibly a glioma; the perfusion and diffusion features are concerning for a malignant tumor.

Histological diagnosis: Diffuse midline glioma, H3 K27 M mutant (WHO IV).

Conclusion

A systematic approach to assessing lesion location, extent, and morphology as well as considering clinical features (age, symptoms, prior therapy) is recommended in the work up of brain tumors. Several clinical and neuroradiological clues will lead to the consideration of non-neoplastic differential diagnosis. Appropriate use of anatomical and advanced scan protocols can maximize the diagnostic value and serial reproducibility of brain tumor imaging.

References

Clarke C, Howard R, Rossor M, Shorvon S, editors. Neurology: a Queen Square textbook. 2nd ed. Oxford: Wiley Blackwell; 2016.

Comelli I, Lippi G, Campana V, Servadei F, Cervellin G. Clinical presentation and epidemiology of brain tumors firstly diagnosed in adults in the emergency department: a 10-year, single center retrospective study. Ann Transl Med. 2017;5(13):269.

Crocetti E, Trama A, Stiller C, Caldarella A, Soffietti R, Jaal J, et al. RARECARE working group. Epidemiology of glial and non-glial brain tumours in Europe. Eur J Cancer. 2012;48(10):1532–42.

Ellingson B, Bendszus M, Boxerman J, Barboriak D, Erickson BJ, Smits M, et al. Consensus recommendations for a standardized brain tumor imaging protocol in clinical trials. Neuro-Oncology. 2015;17(9):1188–98.

Louis DN, Perry A, Reifenberger G, von Deimling A, Figarella-Branger D, Cavenee WK, Ohgaki H, Wiestler OD, Kleihues P, Ellison DW. The 2016 World Health Organization classification of Tumours of the central nervous system: a summary. Acta Neuropathol. 2016;131(6):803–20.

Nunes RH, Hsu CC, da Rocha AJ, do Amaral LLF, Godoy LFS, Waltkins TW. Multinodular vacuolating glioneuronal tumor of the cerebrum: a new "leave me alone" lesion with a characteristic imaging pattern. AJNR Am J Neuroradiol. 2017;38(10):1899–904.

Osborn A, Salzman KL, Jhaveri MD, Barkovich AJ. Diagnostic brain. 3rd ed. Philadelphia: Elsevier; 2016.

Thom M, Liu J, Bongaarts A, Reinten RJ, Paradiso B, Jäger HR, Reeves C, Somani A, An S, Marsdon D, McEvoy A, Miserocchi A, Thorne L, Newman F, Bucur S, Honavar M, Jacques T, Aronica E. Multinodular and vacuolating tumors in epilepsy: dysplasia or neoplasia? Brain Pathol. 2018;28(2):155–71.

Thust SC, Heiland S, Falini A, Jäger HR, Waldman AD, Sundgren PC, Godi C, Katsaros VK, Ramos A, Bargallo N, Vernooij MW, Yousry T, Bendszus M, Smits M. Glioma imaging in Europe: a survey of 220 centres and recommendations for best clinical practice. Eur Radiol. 2018;28(8):3306–17.

Verburg N, Hoefnagels FWA, Barkhof F, Boellaard R, Goldman S, Guo J, Heimans JJ, Hoekstra OS, Jain R, Kinoshita M, Pouwels PJW, Price SJ, Reijneveld JC, Stadlbauer A, Vandertop WP, Wesseling P, Zwinderman AH, De Witt Hamer PC. Diagnostic accuracy of neuroimaging to delineate diffuse gliomas within the brain: a meta-analysis. AJNR Am J Neuroradiol. 2017;38(10):1884–91.

Welker K, Boxerman J, Kalnin A, Kaufmann T, Shiroshi M, Wintermark M. ASFNR recommendations for clinical performance of MR dynamic susceptibility contrast perfusion imaging of the brain. AJNR Am J Neuroradiol. 2015;36(6):E41–51.

Further Reading

Alentorn A, Hoang-Xuan K, Mikkelsen T. Presenting signs and symptoms in brain tumors. Handb Clin Neurol. 2016;134:19–26.

Anderson MD, Colen RR, Tremont-Lukats IW. Imaging mimics of primary malignant tumors of the central nervous system (CNS). Curr Oncol Rep. 2014;16(8):399.

Ly KI, Gerstner ER. The role of advanced Brian tumor imaging in the Care of Patients with central nervous system tumours. Curr Treat Options in Oncol. 2018;19(8):40.

Nandhu H, Wen P, Huang RY. Imaging in neuro-oncology. Ther Adv Neuol Disord. 2018;11:1756286418759865. eCollection 2018

Suh CH, Kim HS, Jung SC, Choi CG, Kim SJMRI. Findings in Tumefactive demyelinating lesions: a systematic review and meta-analysis. AJNR Am J Neuroradiol. 2018;39(9):1643–9.